GSA Data Repository Item 2016363
Liu, H., Wang, Y., Cawood, P.A., and Guo, X., 2016, Episodic slab-rollback and back-arc extension in the Yunnan-Burma region: Insights from Cretaceous Nb-enriched and oceanic-island basalt-like mafic rocks: GSA Bulletin, doi:10.1130/B31604.1.

Supplemental files

***Supplemental file 1** analytical method*

Zircon mineral separates were prepared by conventional heavy liquid and magnetic techniques. Grains were mounted in epoxy, polished and coated with gold and then photographed in transmitted and reflected light. Their internal texture was examined using cathodoluminescence (CL) imaging at the Institute of Geology and Geophysics (IGG), Chinese Academy of Sciences (CAS), Beijing.

Zircon U-Pb ages and trace elements for samples HH-22C and ML-37A were analyzed using a Laser ICP-MS at the IGG CAS. The zircon standards CN92-2, 91500 and GJ were used to calibrate the U-Th-Pb ratios. The standard silicate glass NIST 610 was used to optimize the machine. The spot size for data collection was 30 μm. The errors for individual U-Pb analyses are presented with 1σ error and uncertainties in grouped ages are quoted at 95 % level (2σ). The age calculations and plots were made using Isoplot (version 3.0; Ludwig, 2001). Further detailed descriptions of the instrumentation and analytical procedure for the LA-ICP-MS zircon U-Pb and trace element technique are similar to those described by Yuan et al. (2004).

Measurements of U, Th and Pb for sample HH-22A were conducted using the Cameca IMS-1280 at IGG-CAS. U–Th–Pb ratios were determined relative to the standard zircon Plesˇovice (Sla´ma et al., 2008), and their absolute abundances were calibrated to the standard zircon 91500 (Wiedenbeck et al., 1995), using operating and data processing procedures similar to those described by Li et al. (2009). The weighted mean U–Pb ages and Concordia plots were processed using Isoplot/Ex v.3.0 program (Ludwig, 2001). SIMS zircon U-Pb isotopic data are presented in table 3.

Whole rock samples for geochemistry were crushed to 200-mesh using an agate mill for elemental and Sr-Nd isotopic analyses. The major oxides were analyzed by a wavelength X-ray fluorescence spectrometry at the State Key Laboratory of Isotope Geochemistry, Guangzhou Institute of Geochemistry (GIG), Chinese Academy of Sciences (CAS). Trace element analyses were performed at the GIG CAS by a Perkin-Elmer Sciex ELAN 6000 ICP-MS. Detailed sample preparation and analytical procedure followed Li et al. (2002). Sr, Nd isotopic analyses were carried out at the GIG CAS on a Neptune Plus (Thermo Fisher Scientific, MA, USA) multi-collection mass spectrometry equipped with nine Faraday cup collectors and eight ion counters. Details analytical methods are presented by Yang et al. (2006). Normalizing factors used to correct the mass fractionation of Sr and Nd during the measurements were $^{86}Sr/^{88}Sr = 0.1194$ and $^{146}Nd/^{144}Nd = 0.7219$ (Yang et al., 2005, 2007).

References

Li, X.H., Li, Z.X., Zhou, H.W., Liu, Y., Kinny, P.D., 2002. U-Pb zircon geochronology,

geochemistry and Nd isotopic study of Neoproterozoic bimodal volcanic rocks in the Kangdian Rift of South China: implications for the initial rifting of Rodinia. Precambrian Research 113, 135-154.

Li, X. H., Liu, Y., Li, Q. L., Guo, C. H., and Chamberlain, K. R., 2009. Precise determination of Phanerozoic zircon Pb/Pb age by multicollector SIMS without external standardization. Geochemistry, Geophysics, Geosystems 10, 2415-2440.

Ludwig, K.R., 2001. Sqiud 1.02:A User Manual. Berkeley:Berkeley Geochronological Center Special publication, 1-219.

Sla´ma, J., Kosler, J., Condon, D. J., Crowley, J. L., Gerdes, A., Hanchar, J. M., Horstwood, M. S. A., Morris,G. A., Nasdala, L., Norberg, N., Schaltegger, U., Schoene, B., Tubrett, M. N., and Whitehouse, M. J., 2008. Plesˇovice zircon-A new natural reference material for U-Pb and Hf isotopic microanalysis. Chemical Geology 249, 1-35.

Wiedenbeck, M., Alle, P., Corfu, F., Griffin, W. L., Meier, M., Oberli, F., Von Quadt, A., Roddick, J. C., and Speigel, W., 1995, Three Natural Zircon Standards for U-Th-Pb, Lu-Hf, Trace-Element and REE Analyses. Geostandards Newsletter 19, 1-23.

Yang, J.H., Wu, F.Y., Shao, J.A., Wilde, S.A., Xie, L.W., Liu, X.M., 2006. Constraints on the timing of uplift of the Yanshan Fold and Thrust Belt, North China. Earth and Planetary Science Letters 246, 336-352.

Yuan, H.L., Gao, S., Liu, X.M., Li, H.M., Gunther, D., Wu, F.Y., 2004. Accurate U-Pb age and trace element determinations of zircon by laser ablation-inductively coupled plasma-mass spectrometry. Geostandards and Geoanalytical Research 28, 353-370.

Yang, Y.H., Zhang, H.F., Wu, F.Y., Xie, L.W., Zhang, Y.B., 2005. Accurate Measurement of Strontium Isotopic Composition by Neptune Multiple Collector Inductively Coupled Plasma Mass Spectrometry. Journal of Chinese Mass Spectrometry Society 26, 215-221 (in Chinese with English abstract).

Yang, Y.H., Zhang, H.F., Xie, L.W., Wu, F.Y., 2007. AccurateMeasurement ofNeodym ium Isotopic Composition Using Neptune Multiple Collector Inductively Coupled P lasmaMass Spectrometry. Chinese Journal of Analytical Chemistry 1, 71-74 (in Chinese with English abstract).

Supplemental file 2 *LA-ICPMS Zircon U-Pb dating results for the Mili diabase and Nb-enriched Yaoshan amphibolite*

Analysis	$^{207}Pb/^{235}U$		$^{206}Pb/^{238}U$		$^{207}Pb/^{235}U$		$^{206}Pb/^{238}U$		Th/U
	Ratio	1σ	Ratio	1σ	Age (Ma)	1σ	Age (Ma)	1σ	
Mili Diabase									
ML-37A-01	0.783646	0.039433	0.092305	0.001281	587.6	22.5	569.2	7.6	1.62
ML-37A-02	0.144119	0.008433	0.021942	0.000344	136.7	7.5	139.9	2.2	0.67
ML-37A-03	0.149554	0.009466	0.021987	0.000399	141.5	8.4	140.2	2.5	0.71
ML-37A-04	0.152583	0.009120	0.022105	0.000363	144.2	8.0	140.9	2.3	2.27
ML-37A-05	0.152287	0.011403	0.021698	0.000448	143.9	10.0	138.4	2.8	1.31
ML-37A-06	0.149994	0.010147	0.021241	0.000366	141.9	9.0	135.5	2.3	1.11
ML-37A-07	0.163108	0.017414	0.021295	0.000601	153.4	15.2	135.8	3.8	0.77
ML-37A-08	0.917722	0.036919	0.108403	0.001412	661.2	19.6	663.5	8.2	1.27
ML-37A-09	0.255501	0.011107	0.036878	0.000432	231.0	9.0	233.5	2.7	0.15
ML-37A-10	0.157616	0.004996	0.021792	0.000664	148.6	4.4	139.0	4.2	0.76
ML-37A-11	0.151053	0.004704	0.022047	0.000674	142.8	4.1	140.6	4.3	0.61
ML-37A-12	0.150754	0.004669	0.022003	0.000680	142.6	4.1	140.3	4.3	0.40
ML-37A-13	0.173267	0.005780	0.021801	0.000674	162.2	5.0	139.0	4.3	0.40
ML-37A-14	0.150057	0.004691	0.021960	0.000677	142.0	4.1	140.0	4.3	0.75
ML-37A-15	0.149150	0.004603	0.021907	0.000668	141.2	4.1	139.7	4.2	0.99
ML-37A-16	0.150145	0.004668	0.022008	0.000679	142.0	4.1	140.3	4.3	1.10
ML-37A-17	0.902077	0.027593	0.099337	0.003027	652.8	14.7	610.5	17.7	1.84
Nb-enriched Yaoshan amphibolite									
HH-22C-1	0.128530	0.032980	0.011130	0.001320	71.3	8.4	122.8	29.7	0.16
HH-22C-2	0.074250	0.041940	0.010140	0.001170	65.0	7.5	72.7	39.6	0.10
HH-22C-3	0.077910	0.052220	0.010650	0.002020	68.3	12.9	76.2	49.2	0.19
HH-22C-4	0.086060	0.065010	0.010860	0.001940	69.6	12.4	83.8	60.8	0.22
HH-22C-5	0.083580	0.034990	0.010170	0.001280	65.2	8.1	81.5	32.8	0.19
HH-22C-6	0.073240	0.022410	0.010870	0.000950	69.7	6.0	71.8	21.2	0.12
HH-22C-7	0.033570	0.029890	0.010690	0.001140	68.6	7.3	33.5	29.4	0.12
HH-22C-8	0.051100	0.039730	0.010360	0.001360	66.4	8.7	50.6	38.4	0.24
HH-22C-9	0.062780	0.023540	0.010690	0.001020	68.5	6.5	61.8	22.5	0.21
HH-22C-10	0.043230	0.022230	0.010350	0.000840	66.4	5.4	43.0	21.6	0.16
HH-22C-11	0.046400	0.029170	0.011700	0.001060	75.0	6.8	46.1	28.3	0.05
HH-22C-12	0.084560	0.023050	0.010750	0.000890	68.9	5.7	82.4	21.6	0.11
HH-22C-13	0.075350	0.023950	0.010340	0.001090	66.3	7.0	73.8	22.6	0.19
HH-22C-14	0.121720	0.039400	0.010620	0.001220	68.1	7.8	116.6	35.7	0.12
HH-22C-15	0.073340	0.027730	0.010590	0.000960	67.9	6.1	71.9	26.2	0.13

Supplemental file 3 *SIMS Zircon U-Pb dating results for the OIB-like Yaoshan amphibolite*

Sample/spot#	$^{207}Pb/^{235}U$		$^{206}Pb/^{238}U$		$^{207}Pb/^{235}U$		$^{206}Pb/^{238}U$		207-corr		Th/U
	Ratio	1σ	Ratio	1σ	age (Ma)	1σ	age (Ma)	1σ	age (Ma)	1σ	
HH-22A@02	0.041869	8.64	0.00659	1.73	41.6	3.5	42.3	0.7	42.4	0.7	0.038
HH-22A@03	0.086422	5.73	0.01214	1.74	84.2	4.6	77.8	1.3	77.4	1.4	0.240
HH-22A@04	0.075277	5.56	0.01161	1.58	73.7	4.0	74.4	1.2	74.5	1.2	0.239
HH-22A@05	0.052046	14.90	0.00826	1.81	51.5	7.5	53.0	1.0	53.1	1.0	0.081
HH-22A@06	0.084666	4.30	0.01230	1.68	82.5	3.4	78.8	1.3	78.6	1.3	0.034
HH-22A@07	0.081404	6.31	0.01171	1.57	79.5	4.8	75.0	1.2	74.8	1.2	0.136
HH-22A@08	0.068483	4.76	0.01055	1.69	67.3	3.1	67.7	1.1	67.7	1.1	0.314
HH-22A@09	0.077736	5.11	0.01179	1.61	76.0	3.7	75.5	1.2	75.5	1.2	0.356
HH-22A@1	0.075470	7.32	0.01208	1.68	73.9	5.2	77.4	1.3	77.6	1.3	0.112
HH-22A@10	0.076549	4.23	0.01153	1.59	74.9	3.1	73.9	1.2	73.8	1.2	0.153
HH-22A@11	0.074173	3.73	0.01055	1.77	72.7	2.6	67.7	1.2	67.4	1.2	0.150
HH-22A@12	0.106336	9.73	0.01630	1.95	102.6	9.5	104.2	2.0	104.3	2.0	0.029
HH-22A@13	0.038918	12.49	0.00702	2.01	38.8	4.8	45.1	0.9	45.5	0.9	0.117
HH-22A@14	0.076404	5.88	0.01234	1.67	74.8	4.2	79.1	1.3	79.4	1.3	0.141
HH-22A@15	0.039418	9.58	0.00519	2.13	39.3	3.7	33.3	0.7	33.0	0.7	0.052
HH-22A@16	0.070405	5.90	0.01122	1.59	69.1	3.9	71.9	1.1	72.1	1.2	0.291
HH-22A@17	0.058697	5.95	0.01008	1.60	57.9	3.4	64.7	1.0	65.1	1.0	0.410
HH-22A@18	0.034662	36.12	0.00634	2.93	34.6	12.4	40.8	1.2	41.1	1.2	0.241
HH-22A@19	0.114426	6.35	0.01503	1.57	110.0	6.6	96.2	1.5	95.3	1.5	0.112
HH-22A@20	0.079333	7.17	0.01179	1.62	77.5	5.4	75.6	1.2	75.4	1.2	0.052
HH-22A@21	0.089982	19.96	0.01118	2.00	87.5	16.9	71.7	1.4	70.6	1.9	0.119
HH-22A@22	0.063825	16.75	0.00867	1.89	62.8	10.3	55.7	1.0	55.2	1.1	0.156
HH-22A@23	0.082653	8.70	0.01154	1.60	80.6	6.8	74.0	1.2	73.5	1.2	0.297
HH-22A@24	0.077127	24.51	0.00989	2.17	75.4	18.0	63.4	1.4	62.6	1.5	0.114
HH-22A@25	0.076333	6.54	0.01195	1.61	74.7	4.7	76.6	1.2	76.7	1.2	0.040
HH-22A@26	0.027394	48.06	0.00614	2.57	27.4	13.1	39.5	1.0	40.2	0.9	0.044
HH-22A@27	0.080762	5.48	0.01230	1.73	78.9	4.2	78.8	1.4	78.8	1.4	0.386
HH-22A@28	0.086661	6.60	0.01138	1.70	84.4	5.4	72.9	1.2	72.2	1.2	0.276
HH-22A@29	0.074483	4.72	0.01140	1.66	72.9	3.3	73.1	1.2	73.1	1.2	0.141

Supplemental file 4 *Major oxides and elemental analyzed results*

Sample	10HH-22A	10HH-22B	10HH-22C	10HH-22D	10HH-22E	10HH-22P	10HH-22L	11ML-37A	11ML-37B	11ML-37E	11ML-37F	11ML-37K	11ML-37N	11ML-37Z	Dalongkai
	OIB-like amphibolite		Nb-enriched amphibolite					Nb-enriched diabase							Pl-pyroxunite
SiO_2	47.53	46.07	47.81	45.64	44.32	44.03	51.14	48.29	48.76	49.55	48.93	48.53	49.05	48.63	39.50
TiO_2	3.32	3.27	1.50	1.19	1.48	1.51	0.74	1.86	1.95	1.87	1.77	1.89	1.83	1.53	0.63
Al_2O_3	12.62	13.68	13.31	12.09	13.58	13.83	15.76	13.68	13.11	13.00	13.25	13.08	12.96	13.30	5.47
Fe_2O_3t	15.66	15.65	12.60	11.52	12.47	13.25	10.86	13.33	14.14	13.61	12.97	13.90	13.21	12.04	14.00
MnO	0.20	0.20	0.17	0.15	0.15	0.18	0.17	0.20	0.20	0.18	0.20	0.20	0.19	0.20	0.26
MgO	6.66	6.52	8.29	13.17	10.78	9.83	6.52	5.95	5.63	5.35	5.70	5.63	5.45	6.12	26.62
CaO	10.33	10.58	13.00	13.16	13.99	14.35	12.73	10.89	10.84	11.63	12.41	10.76	12.21	12.62	4.08
Na_2O	2.13	2.34	2.17	1.34	1.19	1.26	1.38	2.42	1.81	1.64	1.82	2.25	1.36	2.28	0.55
K_2O	0.67	0.73	0.50	0.71	0.84	0.64	0.42	0.07	0.08	0.07	0.08	0.12	0.13	0.04	0.24
P_2O_5	0.47	0.47	0.10	0.10	0.15	0.20	0.08	0.20	0.21	0.20	0.19	0.20	0.20	0.16	0.09
L.O.I	0.29	0.38	0.43	0.70	0.83	0.69	0.05	2.29	2.33	1.99	1.82	2.61	2.53	2.34	7.07
Total	99.88	99.89	99.88	99.78	99.77	99.77	99.83	99.18	99.07	99.08	99.16	99.18	99.12	99.26	98.50
P	2053	2035	455	441	649	880	334	877	913	876	845	892	875	718	391
K	4446	4833	3269	4695	5521	4236	2752	489	530	447	550	795	831	250	2024
Sc	29.8	28.7	46.9	41.0	43.7	40.6	43.8	36.6	36.0	37.3	35.7	38.1	37.7	39.1	16.4
Ti	19438	18928	8898	6894	8290	7873	8670	11172	11669	11202	10615	11358	10955	9159	3778
V	373	359	322	262	299	270	280	341	339	337	321	317	317	324	141
Cr	185	181	437	1735	668	527	571	84.9	88.7	84.9	86.8	93.6	81.8	117	1994
Co	49.3	45.1	54.3	66.4	52.8	59.2	59.2	36.5	41.9	35.3	36.6	42.6	33.4	40.2	119
Ni	98.5	89.7	140	477	191	204	233	45.6	47.0	41.5	47.8	48.8	49.3	58.1	1018
Cu	95.8	128	79.2	41.3	61.1	8.57	12.4	44.9	42.8	39.4	30.7	42.4	40.0	24.0	40.2
Zn	136	129	87.0	78.3	79.0	91.6	85.8	132	136	106	114	129	113	103	171

Sample	10HH-22A	10HH-22B	10HH-22C	10HH-22D	10HH-22E	10HH-22P	10HH-22L	11ML-37A	11ML-37B	11ML-37E	11ML-37F	11ML-37K	11ML-37N	11ML-37Z	Dalongkai
	OIB-like amphibolite		Nb-enriched amphibolite					Nb-enriched diabase							Pl-pyroxunite
Ga	22.3	21.2	15.3	14.1	16.2	16.1	16.3	23.2	18.9	19.9	21.1	18.5	22.1	19.6	7.56
Rb	11.6	16.3	8.6	35.2	41.5	17.8	23.6	1.19	1.36	1.15	1.35	1.54	3.22	0.430	7.76
Sr	416	485	368	184	255	435	450	229	234	278	272	233	278	288	74.6
Y	36.4	34.2	18.6	14.7	18.1	18.3	20.0	37.0	39.5	37.3	35.4	39.8	35.3	30.3	11.1
Zr	201	186	68.6	60.5	75.4	76.0	80.0	133	141	135	129	140	127	102	45.4
Nb	26.0	20.0	8.56	7.95	8.94	10.6	12.3	8.89	9.66	8.96	8.70	9.41	8.71	7.20	1.59
Cs	1.01	1.83	2.26	4.55	5.45	3.59	3.73	0.030	0.050	0.030	0.030	0.050	0.080	0.030	9.26
Ba	264	296	94.7	104	121	100	110	21.2	23.1	15.2	15.2	33.3	22.8	10.8	58.2
La	25.8	28.9	5.78	5.87	7.17	6.75	7.50	9.99	11.0	10.1	10.1	10.5	10.2	8.67	2.84
Ce	62.8	64.8	13.9	13.8	16.7	16.1	17.5	22.5	25.0	23.1	22.1	24.4	23.5	19.7	7.34
Pr	8.99	8.59	2.07	1.94	2.34	2.27	2.49	3.21	3.44	3.33	3.09	3.38	3.20	2.70	1.00
Nd	40.1	37.8	9.68	9.13	11.0	10.5	11.5	16.1	16.8	16.3	14.9	16.5	15.8	13.0	4.88
Sm	8.67	8.06	2.66	2.45	2.91	2.79	3.04	4.81	5.01	4.94	4.58	4.92	4.62	3.86	1.41
Eu	2.91	2.59	0.907	0.871	1.14	0.985	1.08	1.73	1.61	1.63	1.52	1.57	1.50	1.37	0.477
Gd	8.23	7.88	2.96	2.62	3.25	3.10	3.40	5.49	5.65	5.44	5.02	5.46	5.32	4.51	1.52
Tb	1.31	1.19	0.545	0.457	0.565	0.544	0.606	1.04	1.09	1.02	0.994	1.07	1.00	0.832	0.292
Dy	7.02	6.62	3.21	2.69	3.36	3.33	3.61	7.01	7.21	6.77	6.50	6.85	6.67	5.50	1.90
Ho	1.38	1.28	0.653	0.535	0.668	0.675	0.732	1.33	1.37	1.29	1.21	1.34	1.3	1.06	0.366
Er	3.28	3.07	1.71	1.33	1.65	1.70	1.85	3.89	4.11	3.85	3.55	3.88	3.70	3.09	1.05
Tm	0.466	0.432	0.251	0.207	0.245	0.257	0.276	0.570	0.630	0.550	0.520	0.570	0.540	0.460	0.148
Yb	2.86	2.71	1.64	1.34	1.63	1.69	1.83	3.50	3.87	3.49	3.25	3.70	3.37	2.90	0.964
Lu	0.440	0.418	0.261	0.211	0.262	0.275	0.290	0.562	0.594	0.541	0.509	0.562	0.551	0.456	0.155
Hf	4.65	4.25	1.63	1.57	1.87	1.82	1.91	3.54	3.81	3.69	3.39	3.74	3.59	2.81	1.07
Ta	1.47	1.18	0.498	0.510	0.563	0.583	0.674	0.570	0.600	0.580	0.550	0.600	0.550	0.450	0.114

Sample	10HH-22A	10HH-22B	10HH-22C	10HH-22D	10HH-22E	10HH-22P	10HH-22L	11ML-37A	11ML-37B	11ML-37E	11ML-37F	11ML-37K	11ML-37N	11ML-37Z	Dalongkai
	OIB-like amphibolite		Nb-enriched amphibolite					Nb-enriched diabase							Pl-pyroxunite
Pb	4.18	4.18	4.14	2.96	5.68	3.65	5.31	5.41	4.61	5.95	7.52	4.43	5.79	4.53	7.57
Th	2.20	3.68	0.888	0.894	1.20	0.918	1.14	1.28	1.33	1.29	1.24	1.31	1.23	1.13	0.330
U	0.400	0.383	0.202	0.387	0.423	0.236	0.266	0.400	0.420	0.420	0.360	0.580	0.320	0.370	0.182

Dalongkai samples are from Liu et al. (under review-a)

References

Liu, H. C., Wang, Y. J., Guo, X. F., Fan, W. M., and Song, J. J., under review-a. Late Triassic post-collisional slab break-off along the Ailaoshan suture: insights from OIB-like metagabbros and associated rocks. Int J Earth Sci.

Supplemental file 5 Sr-Nd isotopic compositions

Sample	**10HH-22C**	**10HH-22E**	**10HH-22G**	**11ML-37A**	**11ML-37B**	**11ML-37E**	**11ML-37Z**	**11ML-18A**	**11ML-18e**	**11ML-19A**	**11ML-19B**	**10HH-67A**	**10HH-67D**	**10HH-69E**
Ref.				**This study**				**Dalongkai mafic rocks (Liu et al., under review-b)**				**~810 Ma amphibolites (Cai et al., 2014)**		
Age (Ga)	0.07	0.07	0.07	0.07	0.07	0.07	0.07	0.07	0.07	0.07	0.07	0.07	0.07	0.07
Rb	8.59	41.50	11.56	1.19	1.36	1.15	0.43	10.40	4.56	6.86	3.96	5.11	2.12	12.73
Sr	368.10	255.10	416.20	229.00	234.00	278.00	288.00	104.00	52.00	333.00	217.00	457.70	297.50	242.40
Rb/Sr	0.02	0.16	0.03	0.01	0.01	0.00	0.00	0.10	0.09	0.02	0.02	0.01	0.01	0.05
$^{87}Rb/^{86}Sr$	0.067462	0.470600	0.080345	0.015032	0.016813	0.011966	0.004319	0.289269	0.253680	0.059588	0.052788	0.032313	0.020569	0.152015
$^{87}Sr/^{86}Sr$	0.704890	0.705645	0.705421	0.705120	0.706011	0.705335	0.705128	0.705368	0.705879	0.704820	0.705343	0.706913	0.707234	0.712167
2s	11	12	9	14	17	14	13	15	16	11	10	13	13	12
$(^{87}Sr/^{86}Sr)_i$	0.704823	0.705177	0.705341	0.705105	0.705994	0.705323	0.705124	0.705080	0.705627	0.704761	0.705291	0.706880	0.707213	0.712016
$(^{87}Sr/^{86}Sr)_{CHUR}$	0.704419	0.704419	0.704419	0.704419	0.704419	0.704419	0.704419	0.704419	0.704419	0.704419	0.704419	0.704419	0.704419	0.704419
e_{Sr}	5.73	10.76	13.09	9.73	22.37	12.83	10.01	9.39	17.15	4.86	12.38	34.94	39.67	107.85
Sm	2.66	2.91	8.67	4.81	5.01	4.94	3.86	1.51	1.33	4.03	4.92	5.58	5.09	5.61
Nd	9.68	10.95	40.12	16.10	16.80	16.30	13.00	5.37	4.73	13.80	17.40	27.17	24.56	27.38
$^{147}Sm/^{144}Nd$	0.166084	0.160615	0.130652	0.180585	0.180237	0.183041	0.179698	0.170225	0.170445	0.176643	0.171108	0.124223	0.125264	0.123777
$^{143}Nd/^{144}Nd$	0.512808	0.512817	0.512810	0.512777	0.512698	0.512733	0.512746	0.512703	0.512777	0.512802	0.512809	0.512476	0.512476	0.512457
2s	8	12	6	8	7	9	7	30	19	7	5	8	6	8
T_{CHUR}(Ga)	-0.85	-0.76	-0.40	-1.33	-0.56	-1.07	-0.97	-0.38	-0.81	-1.25	-1.03	0.34	0.35	0.38
T_{DM}(Ga)	1.10	0.96	0.63	1.72	2.06	2.08	1.82	1.57	1.32	1.44	1.22	1.15	1.16	1.18
$(^{143}Nd/^{144}Nd)_i$	0.512732	0.512743	0.512750	0.512695	0.512615	0.512650	0.512664	0.512625	0.512699	0.512721	0.512731	0.512419	0.512419	0.512400
$(^{143}Nd/^{144}Nd)_{CHUR}$	0.512548	0.512548	0.512548	0.512548	0.512548	0.512548	0.512548	0.512548	0.512548	0.512548	0.512548	0.512548	0.512548	0.512548
$\varepsilon_{Nd}(t)$	3.59	3.81	3.95	2.86	1.32	1.98	2.26	1.50	2.94	3.37	3.57	-2.51	-2.52	-2.88

References

Liu, H. C., Wang, Y. J., and Zi, J. W., under review-b. Petrogenesis of the Dalongkai mafic-ultramafic intrusion and its tectonic implication for the Paleotethyan evolution in

the Ailaoshan tectonic zone (SW China). J. Asian Earth Sci.

Cai, Y. F., Wang, Y. J., Cawood, P. A., Fan, W. M., Liu, H. C., Xing, X. W., and Zhang, Y. Z., 2014. Neoproterozoic subduction along the Ailaoshan zone, South China: Geochronological and geochemical evidence from amphibolite. Precambrian Res. 245, 13-28.

Supplemental file 6 *Selected major (wt. %) and trace elements (ppm) versus Zr (ppm) diagrams for checking element mobility during post-intrusive alteration. Symbols are the same as in Figure 10.*

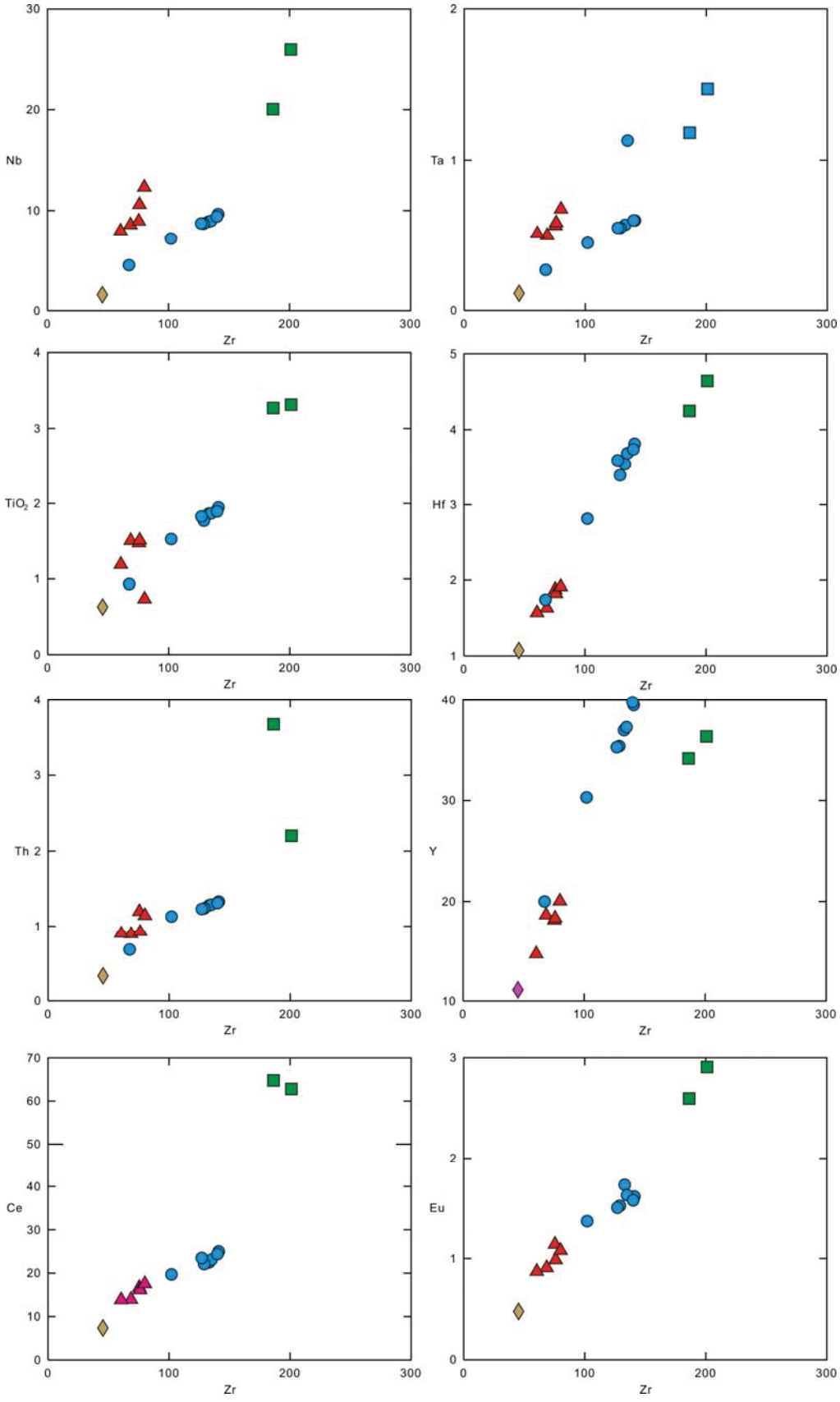

Supplemental file 7 *Nb/La versus MgO (wt. %) diagram. Symbols are the same as in Figure 6A.*

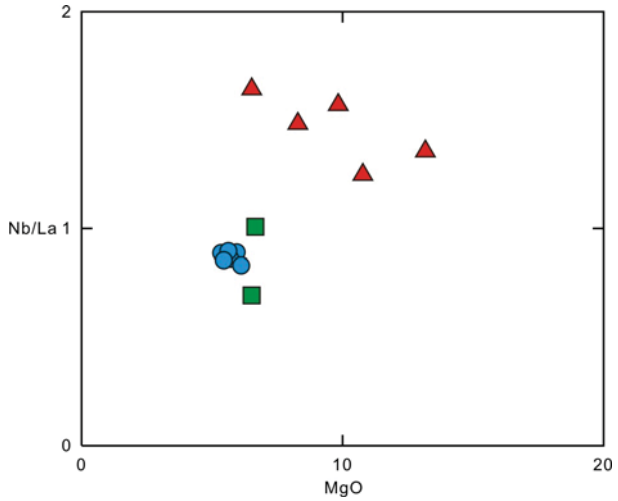

Supplemental file 8 *Selected trace elements (Cr, Ni and Sr; ppm) versus $Mg^{\#}$ diagrams. Symbols are the same as in Figure 10.*

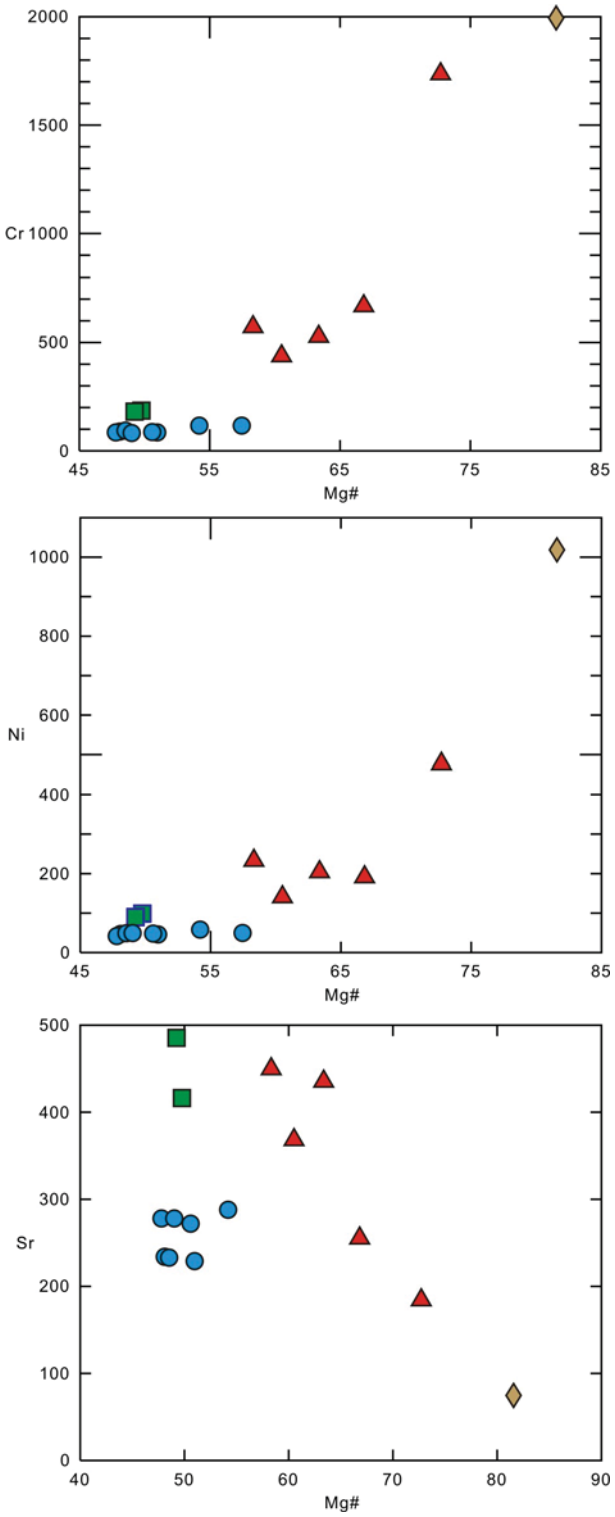

Supplemental file 9 *Selected major elements (wt. %) versus $Mg^{\#}$ diagrams. Symbols are the same as in Figure 10.*

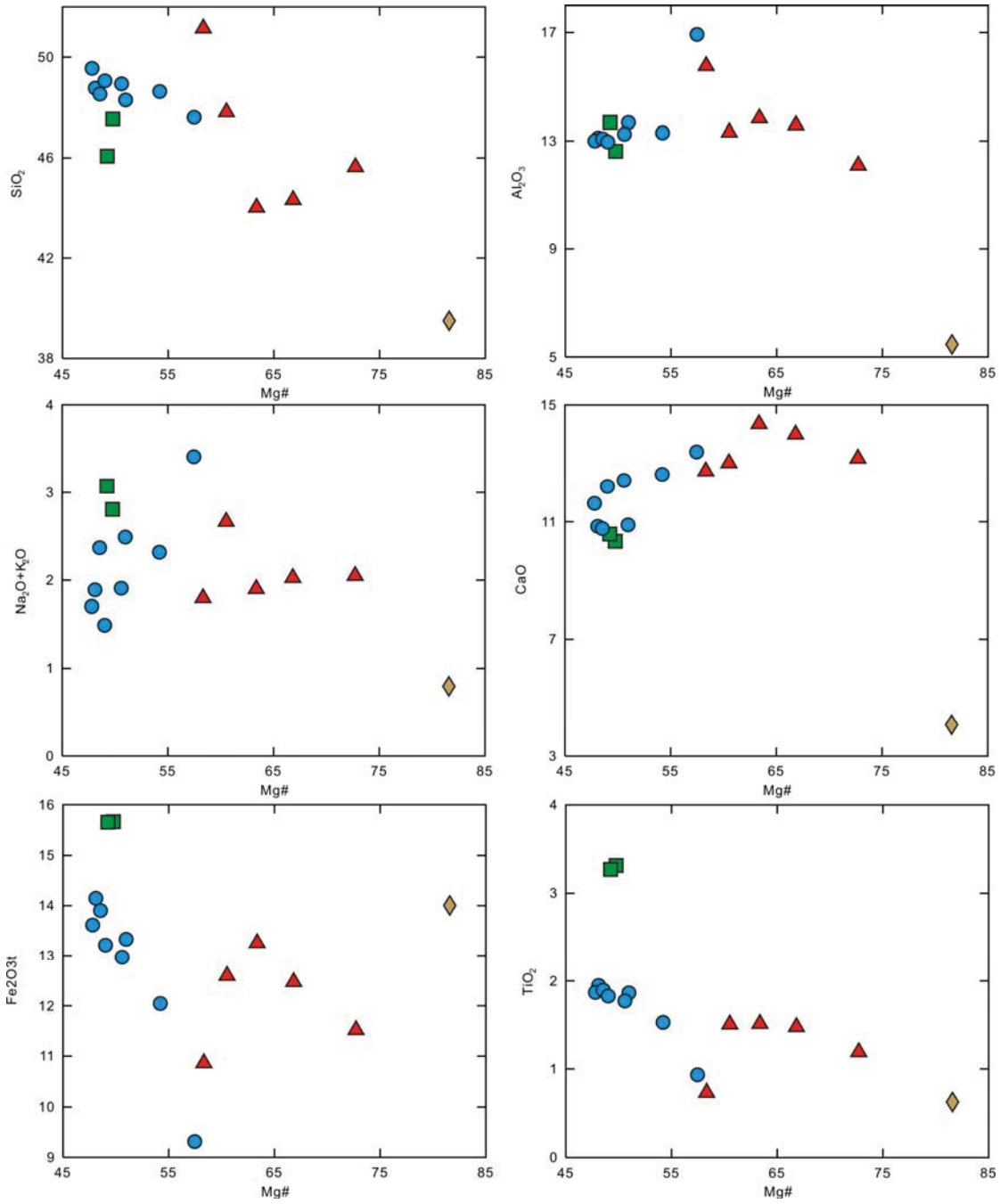

Supplemental file 10 *Sr/Y versus Y diagram (Defant et al., 1993) and La_N/Yb_N versus Yb_N (Martin, 1999) diagrams. Symbols are the same as in Figure 6A.*

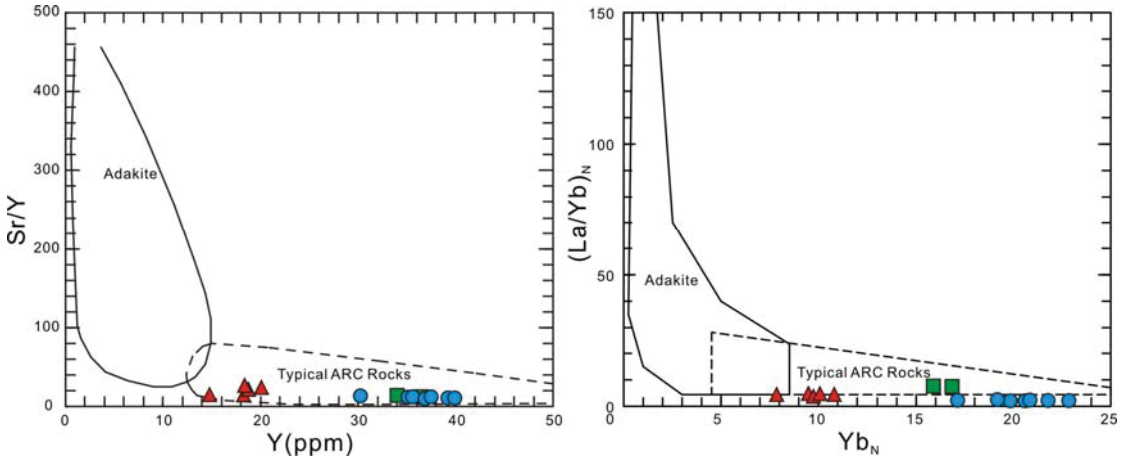

References

Defant, M.J., Drummond, M.S., Mount, S.T.H., 1993. Potential example of the partial melting of the subducted lithosphere in a volcanic arc. Geology, 21(547- 550).

Martin, H., 1999. Adakitic magmas: modern analogues of Archaean granitoids. Lithos, 46(3): 411-429.

Supplemental file 11 *Selected trace elements (ppm) versus Nb diagrams. Symbols are the same as in Figure 6A.*

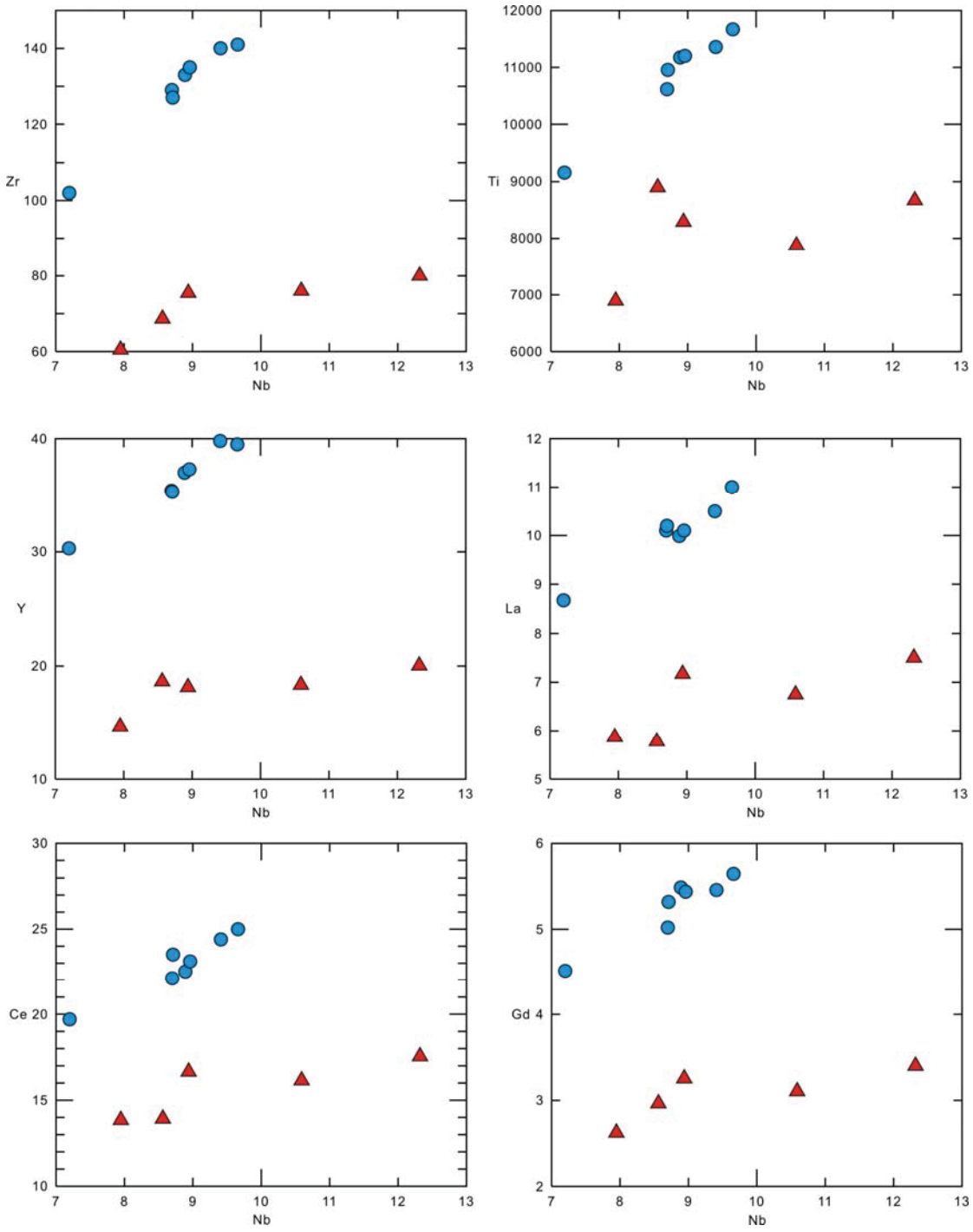

Supplemental file 12 *Ta versus Nb, Zr versus Ta, La versus Nb, TiO_2 versus Zr diagrams. Shown for reference are model curves generated through mixing between the OIB-like (Sample HH-22A from this study) and Arc-like (Dalongkai plagioclase-pyroxenites from Liu et al. under review-b) mantle components. Symbols are the same as in Figure 10.*

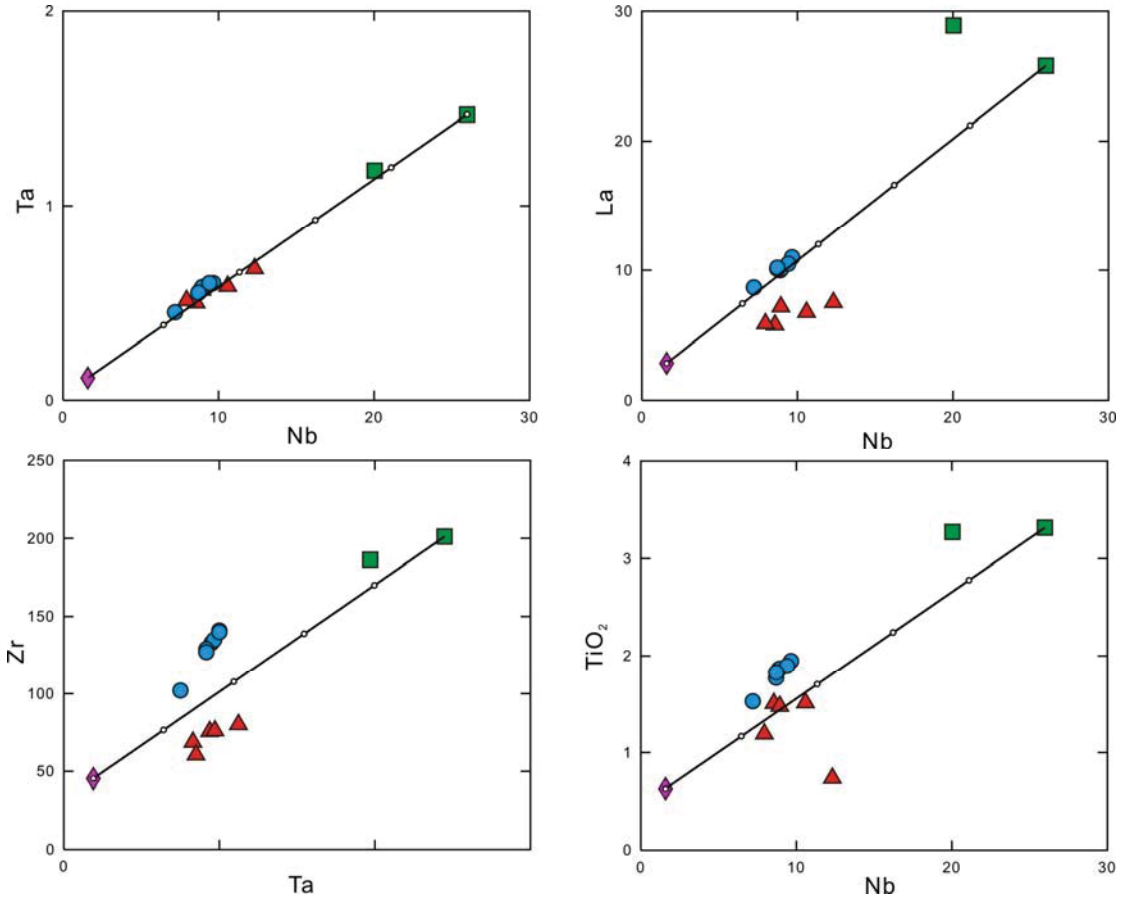

References

Liu, H. C., Wang, Y. J., and Zi, J. W., under review-b. Petrogenesis of the Dalongkai mafic-ultramafic intrusion and its tectonic implication for the Paleotethyan evolution in the Ailaoshan tectonic zone (SW China). J. Asian Earth Sci.

Supplemental file 13 *Tectonic discrimination diagrams involving: (a) Ti/100-Zr-Y*3 (Pearce and Cann, 1973), (b) Cr versus Y (Pearce, 1982). N-MORB: normal mid-oceanic ridge basalt, E-MORB: enriched mid-oceanic ridge basalt, BABB: back-arc basin basalt, OIB: ocean island basalt, IAB: island arc basalt, WPB: within-plate basalt. Symbols are the same as in Figure 6A.*

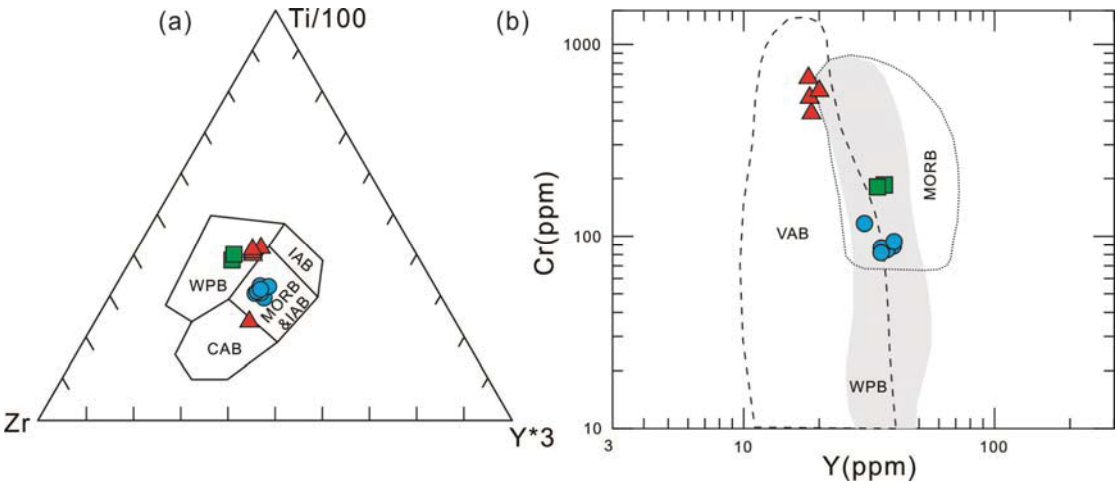

References

Pearce, J.A., 1982. Trace element characteristics of lavas from destructive plate boundaries. In: Thorpe R. S. (ed.). Andesites. Chichester: Wiley: 525-548.

Pearce, J.A., Cann, J.R., 1973. Tectonic setting of basic volcanic rocks determined using trace element analysis. Earrh and Planetary Science Letters, 12: 339-349.